PIEZOELECTRIC NONLINEARITY IN GAN LAMB MODE RESONATORS

Siping Wang, Laura C. Popa, and Dana Weinstein
Massachusetts Institute of Technology, Cambridge, MA, USA

ABSTRACT

This paper reports on the measurement of nonlinearity in GaN Lamb mode resonators subjected to power levels between −10 and +10 dBm. In these devices, nonlinearity manifests itself as both frequency shift ($\Delta f/f$ of 60-128 ppm) and change in motional impedance ($\Delta R_m/R_m$ of 13-33%). In this work, we decouple the contributions from self-heating and strain-induced piezoelectric nonlinearity to $\Delta R_m/R_m$, and conclude that strain-induced change in piezoelectric coefficients Δe_{31} and Δe_{33} is the dominant cause of $\Delta R_m/R_m$, accounting for 31% of the total 33% observed shift. The result is consistent with 2nd order nonlinear coefficients previously derived analytically [1].

KEYWORDS

Piezoelectric nonlinearity; Gallium Nitride; Lamb mode resonator; self-heating; power handling; IIP_3.

INTRODUCTION

High Q, small footprint MEMS resonators have shown exciting promise as building blocks in RF wireless communication, timing, navigation, and sensing applications. Piezoelectric transduction is widely used in these devices as an efficient coupling mechanism. Among the various piezoelectric materials, Wurtzite crystal (AlN [2], ZnO [3], and GaN [4,5]) based devices exhibit large piezoelectric coefficients and excellent mechanical properties. In particular, recent advances in GaN Monolithic Microwave IC (MMIC) technology have made it an attractive platform for the realization of high performance MEMS resonators. With GaN's wide band gap (3.4 eV), high 2DEG mobility, and high piezoelectric coefficients, integration of GaN MEMS with High Electron Mobility Transistors (HEMTs) presents many opportunities for high frequency applications [6,7]. Within this context, the potential for monolithic integration of GaN MEMS resonators with circuits provides important advantages including the elimination of parasitic capacitance and inductance from bond pads and routing, size, weight, and power scaling, and simplification of fabrication and packaging.

Whether for use in radio filters or in frequency references, the resonator's capability to handle large RF power is crucial for system performance. It is therefore important to understand any nonlinearity in piezoelectric MEMS resonators. Studies have shown that self-heating is a primary contributor to frequency shift in AlN Lamb mode resonators [8]. In this paper, we show that GaN Lamb mode resonators (Fig. 1) are subject not only to frequency shift (Δf) from self-heating, but also to an increase in motional impedance (ΔR_m) with increasing power levels due to a significant nonlinearity in piezoelectric coefficients.

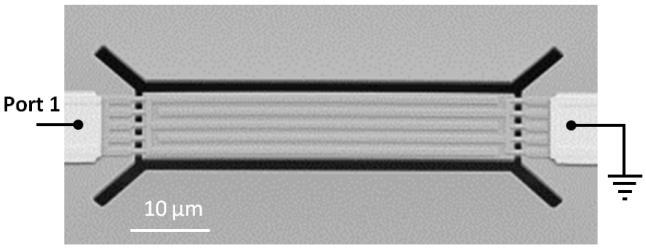

Figure 1: SEM of GaN Lamb mode resonator under study. This corresponds to Device 2 in Figure 3.

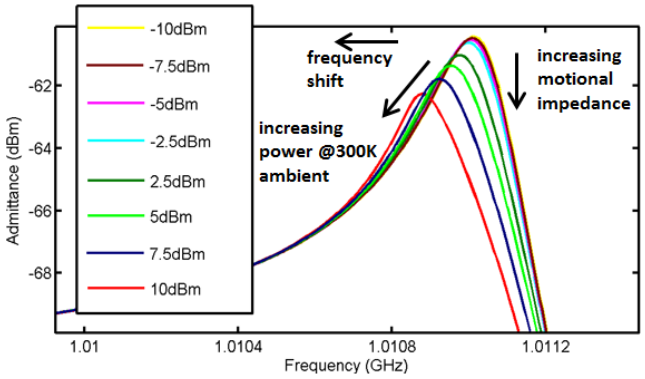

Figure 2: 1-port frequency response of GaN Lamb mode resonator, showing frequency drop and motional impedance increase with increasing power levels.

NONLINEARITY IN GAN RESONATORS

Fig. 2 shows the measured 1-port frequency response of the GaN Lamb mode resonator in Fig. 1 operating at 1.01 GHz, under power levels ranging from -10 dBm to +10 dBm delivered by an Agilent 5225A VNA. Devices were probed under vacuum in a Cascade PMC200, with chuck temperature fixed at 300K. Nonlinear behavior in both frequency and amplitude (or motional impedance) can be seen. Decoupling these contributions to the total nonlinear response is a critical step to managing and designing for maximum power handling in contour mode resonators.

Frequency shift Δf

As RF power increases, resonance frequency shifts, as shown in Fig. 2. There are several possible sources for this behavior. One possibility is an amplitude-induced change in stiffness. In addition, the resonator's temperature may increase due to Joule heating caused by current flowing in the interdigitated transducers (IDTs) on the device. This can also lead to resonance shift through the temperature coefficient of frequency (TC_F), which is a result of the material's temperature dependence of Young's modulus (TC_E).

Table 1: Measured frequency shift at +10dBm input power of three GaN Lamb-wave resonators with different anchoring schemes. This shift is normalized to average mechanical energy density and heat generated to account for differences in amplitude of vibration and thermal conductance for different tethering schemes.

High power @ +10dBm	Device 1	Device 2	Device 3
SEM	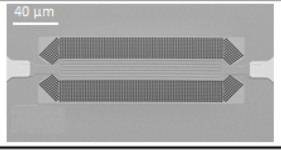	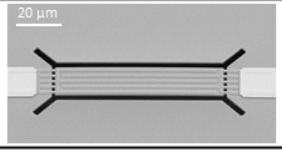	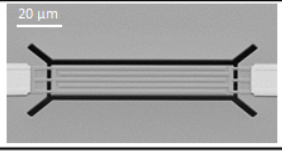
Device Description	PnC resonator (7^{th} harmonic and width is 160um)	5 tethered resonator (5^{th} harmonic and width is 60um)	3 tethered resonator (5^{th} harmonic and width is 60um)
$\Delta f/f$ (ppm) @ 10dBm	60	128	78
$(\Delta f/f)/E_{mech}$(ppm/J·um^2)	1.2e6	1.8e6	2.5e6
$(\Delta f/f)$/Heat (ppm/mW)	3.5e6	7.5e6	9.3e6

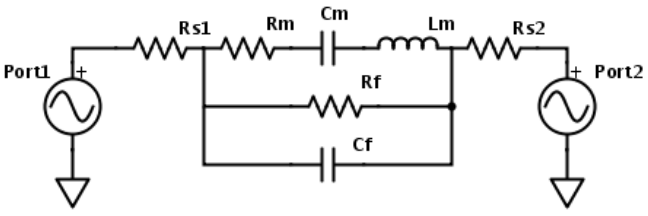

Figure 3: Lumped model equivalent circuit of GaN resonator (R_m, C_m and L_m) with parasitic series resistance R_{S1}, R_{S2} and feed-through capacitance and resistance C_f and R_f.

To pinpoint the root of Δf, we fabricated and measured 3 GaN Lamb mode resonators on the same die, but with different anchoring schemes (Table 1). All 3 devices have the same mode shape, thus each resonators' average mechanical energy density E_{mech}, which represents their vibrational intensity, can be compared directly between devices. Stiffness nonlinearity is an inherent material property and should not depend on device anchoring scheme for a given mode. Therefore, if amplitude-induced change in stiffness were the dominant cause of Δf, then the normalized frequency shift, $(\Delta f/f)/E_{mech}$, would be similar across these devices.

If instead temperature-induced Δf were the dominant cause, then $(\Delta f/f)/Heat$ would be different among the 3 devices, and related to the thermal conductivity defined by the anchoring scheme. Here, $Heat$ is the heat power generated in the resonator. Namely, increasing connection area with the wafer leads to more efficient heat dissipation, lower increase in temperature and consequently, smaller $\Delta f/f$.

The Butterworth van Dyke model for a MEMS resonator was modified to include electrical parasitic resistance and capacitance, as shown in Fig. 3. R_m, C_m and L_m represent the motional branch of the mechanical resonator; R_f and C_f are the feed-through resistance and capacitance, respectively. R_{S1} and R_{S2} are the series resistances associated with the IDT electrodes. The following steps were used to calculate E_{mech} and $Heat$ for the three devices in Table 1.

1. Start with the admittance frequency response at lower power (−10 dBm), prior to the onset of nonlinearity. Fit the frequency response using the equivalent circuit model in Fig. 3 to extract R_f and C_f. R_f is usually an order of magnitude larger than R_m, thus can be ignored when placed in parallel with R_m.
2. Find S_{11}, S_{21} and Z at the peak frequency at +10dBm.
3. Absorbed power at +10dBm can then be calculated: $P_{Absorbed} = P_{VNA}(1 - |S_{11}|^2 - |S_{21}|^2)$. Absorbed power is dominated by mechanical loss through R_m, thus the RMS motional current i_m^2 can be expressed as $2P_{Absorbed}/Re(Z)$.
4. At the peak frequency under +10dBm input power, impedance due to C_m and L_m cancel out, thus only R_m and C_f are left in parallel. Based on the current flowing through R_m, namely i_m^2, we can calculate the current through resonator i^2 (motional and feed-through branches combined).
5. Resonator self-heating is caused by Joule heating due to the RF current flowing in the electrodes. Thus it can be calculated using $Heat = 0.5i^2(R_{S1} + R_{S2})$ Series resistance can be estimated based on electrode material and geometry. In this case, IDTs are made of 100nm of Ni.
6. Motional current is a direct indication of the amplitude of vibration for given resonance frequency and transducer efficiency. Normalizing the motional current i_m^2 by electrode area gives a quantity directly proportional to mechanical energy density. Thus $E_{mech} \propto i_m^2/A_{IDT}$. This normalization is important since Device 1 under study has different width (in the non-resonant dimension) and different number of harmonics than Devices 2 and 3.

Table 1 lists the resulting $(\Delta f/f)/E_{mech}$ and $(\Delta f/f)/Heat$ of the three devices based on this analysis. $(\Delta f/f)/E_{mech}$ varies significantly across the devices under test, inconsistent with the hypothesis that amplitude nonlinearity is the dominant cause for frequency shift. On the other hand,

$(\Delta f/f)/Heat$ shows good consistency with the anchoring scheme, exhibiting a growing trend when going from resonator with 3 tethered anchors on each side to 5 tethered anchors to a PnC design, in which the entire perimeter is connected to the substrate. We conclude that self-heating dominates frequency shift, in agreement with the conclusion reported in AlN [8].

Shift in motional impedance ΔR_m

Just as in the case of Δf, multiple factors contribute to the change in motional impedance ΔR_m. First, contribution from self-heating is parsed out by testing the Device 2 at different ambient temperatures with low input power (−10dBm) where self-heating is negligible. Fig. 4 shows that f reduces and R_m increases with rising temperature, as expected. A TC_F of $-23ppm/K$ and Temperature Coefficient of R_m (TC_{Rm}) of $+275ppm/K$ are obtained from measurement. Using the extracted TC_F, a temperature increase of $\Delta\tau = 6$K at +10 dBm can be derived. This means $\Delta R_m/R_m = TC_{Rm} \cdot \Delta\tau \approx 2\%$ at +10 dBm. Self-heating induces a temperature rise, changing material piezoelectricity, stiffness, permittivity (Δε) and loss (Δb). The combined effect of these changes on $\Delta R_m/R_m$ is around 2%.

Large amplitude of vibration can also change material properties, leading to ΔR_m. Three possible sources of R_m nonlinearity are considered here:

1. *Stiffness dependence.* As discussed in the previous section, amplitude-induced stiffness change (Δc) is negligible compared with temperature-induced stiffness change, thus it does not contribute to ΔR_m either.
2. *Damping dependence.* Under large amplitude resonance, a significant deformation of the suspension structure (tethers or PnC) could result in an amplitude dependence of anchor loss, reducing R_m of the resonator. However, according to COMSOL FEM simulation, the maximum displacement in Device 2 at +10 dBm is less than 3Å. Such small displacement is negligible compared to resonator anchor size, thus should not contribute to Δb.
3. *Piezoelectric coefficients.* After ruling out these two factors, we conclude that the amplitude-induced Δe_{31} and Δe_{33} are the dominant contribution to ΔR_m, consisting about 31% of the total 33% change (Table 2).

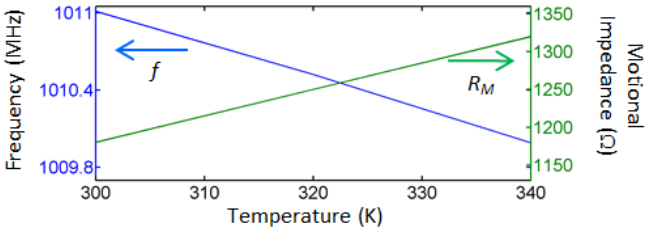

Figure 4: Ambient temperature measurement of Device 2, showing resonance frequency shift and motional impedance increase. The temperature coefficients of frequency and motional impedance are extracted: TC_F=-23ppm/K and TC_{Rm}=+275ppm/K. This indicates Δτ of ~6K when input power is +10dBm, such that $\Delta R_m/R_m$ due to self-heating is ~2%.

Table 2: Possible contributions to $\Delta R_m/R_m$ at high input power. Stiffness c, permittivity ε, damping b, and piezoelectric coefficients e_{33} and e_{31} are considered. Based on measurement, strain-induced piezoelectric nonlinearity is the dominant cause of ΔR_m.

Sources contributing to ΔR_m in Device 2 at +10 dBm	**Contribution to $\Delta R_m/R_m$ (absolute)**	**Comment**
Self-heating → Δe_{31} Δe_{33}	2%	Extracted from thermal measurement (Fig. 4)
Self-heating → Δc		
Self-heating → Δε		
Self-heating → Δb		
Large vibration amplitude → Δc	N/A.	Conclusion from analysis on frequency shift
Large vibration amplitude → Δb	N/A.	The maximum displacement in the resonator is less than 3Å
Large vibration amplitude → Δe_{31} Δe_{33}	31%	Extracted based on the total $\Delta R_m/R_m$ @+10dBm, calculated using measurement (Table 3)
Total $\Delta R_m/R_m$ at +10 dBm	33%	Measured

Amplitude-induced nonlinearity in piezoelectric coefficients is a fundamental material property, independent of resonator harmonic, width, or anchoring scheme. Correspondingly, we expect $\Delta R_m/R_m$ for the three resonators studied here to depend only on vibrational amplitude. Normalizing $\Delta R_m/R_m$ by the intensity of vibration, namely $(\Delta R_m/R_m)/E_{mech}$, should therefore be constant across the three Lamb mode resonators under consideration. The calculated values of $(\Delta R_m/R_m)/E_{mech}$ are listed in Table 3 with good agreement for all devices, verifying that amplitude-induced Δe_{31} and Δe_{33} dominate ΔR_m.

Using theoretical values of the 2nd order nonlinear coefficients of GaN analytically derived in [1] and the simulation results of the device strain at +10 dBm input power, a strain-induced $\Delta R_m/R_m$ of 18%-24% is predicted, not far from the result based on experiment (31%).

Table 3: Increase in motional resistance normalized to average mechanical energy density.

High power @ +10dBm	**Device 1**	**Device 2**	**Device 3**
$\Delta R_m/R_m$ (ppm)	18%	33%	13%
$(\frac{\Delta R_m}{R_m})/E_{mech}$ (ppm/J·um^2)	3.8e3	4.7e3	4.5e3

IIP$_3$ Analysis

In RF communication, the input power at the third-order intercept point, namely IIP_3, is an important specification in weakly nonlinear devices, such as amplifiers

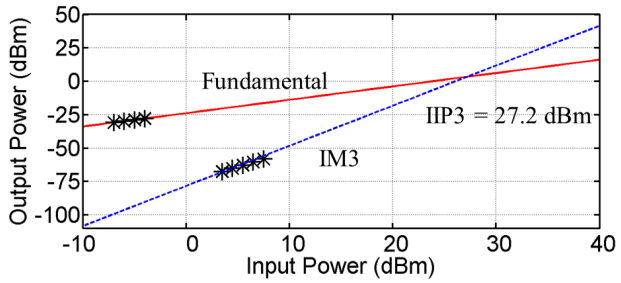

Figure 5: Power handling measurement of Device 1 at 993 MHz, using input tones spaced at 300 kHz and 600 kHz.

and front-end filters, as a metric for power handling. Fig. 5 shows the IP_3 measurement of Device 1, the PnC resonator. Two interfering tones spaced at 300 kHz and 600 kHz below the resonance frequency are superimposed at the resonator port. Due to the nonlinear effects, non-zero energy can be measured at the resonance frequency from the output port. The input power level at which nonlinear output and third-order intermodulation distortion (IM_3) intersect is called IIP_3. A higher IIP_3 indicates better power handling and tolerance to strong interferers, and is therefore a critical metric for filters in RF communication.

As previously discussed, the two dominant nonlinear effects in GaN Lamb mode resonators are self-heating-induced stiffness change (Δc) and amplitude-induced piezoelectric coefficient change (Δe_{31} and Δe_{33}). The piezoelectric equation now takes the following form:

$$T = (c_o + \Delta c)S + (e_o + \Delta e)E$$

where T is the stress field, S is the strain field and E is the electric field. While we can see both effects in the 1-port frequency response of the nonlinear resonators, IP_3 measurement relies on frequency mixing in the 3rd order harmonic terms, and behaves differently for nonlinearity resulting from temperature and amplitude.

We first consider the change in stiffness (Δc), which was previously determined to be dominated by Δτ. In the case of Device 2, based on GaN's thermal conductivity ($1.3\,W/cm℃$), specific heat ($0.49\,J/gK$), density ($6.15\,g/cm^3$), the resonator's volume ($60 \times 20 \times 1.6\,\mu m^3$), and anchoring scheme, the thermal time constant is calculated to be $70\,\mu s$, much longer than the timescale of vibrations ($1\,ns$). Therefore, Δc results from a steady-state temperature change, and is not time dependent. Consequently Δc does not result in frequency mixing leading to IM_3.

We then add the second order nonlinear effect to the piezoelectric coefficient: $e = e_o(1 + \alpha S^2)$ or alternately $e = e_o(1 + \beta E^2)$:

$$T = cS + e_o(1 + \beta E^2)E$$

The two interfering tones $\omega_1 = \omega_o - \Delta\omega$ and $\omega_2 = \omega_o - 2\Delta\omega$ mix in the E^3 nonlinear term, leading to a driving force at $2\omega_1 - \omega_2 = \omega_o$ and resulting in the 3rd order intermodulation distortion. Consequently, we conclude that strain (or amplitude) induced piezoelectric coefficient change (Δe_{31} and Δe_{33}) is the leading component in IM_3 nonlinearity and directly determines the resonator's IIP_3.

CONCLUSION

This paper reports the experimental observation and analysis of nonlinearities in Lamb mode GaN MEMS resonators. We conclude that self-heating is the dominant cause of frequency shift while strain-induced nonlinearity in the piezoelectric coefficients is the dominant mechanism for a significant shift in motional impedance (ΔR_m) when input power increases. This piezoelectric nonlinearity is also the key factor in determining the device IIP_3. These results verify analytical models of piezoelectric nonlinearities and provide a means of predictive design and optimization of RF GaN resonators for frequency sources and filters.

ACKNOWLEDGEMENTS

The authors thank Brian Schultz and Thomas Kazior at Raytheon for GaN growth and process discussions. This work was funded by DRAPA DAHI Foundry N66001-13-1-4022 and NSF Career EECS-1150493.

REFERENCES

[1] P.-Y. Prodhomme, A. Beya-Wakata, G. Bester, "Nonlinear piezoelectricity in Wurtzite semiconductors," *Physical Review B* 88(12), 121304 (2013).
[2] G. Piazza, P.J. Stephanou, A.P. Pisano, "Piezoelectric Aluminum Nitride vibrating contour-mode MEMS resonators," *IEEE JMEMS* 15(6), 1406-18 (2006).
[3] S. Humad, et al., "High frequency micromechanical piezo-on-silicon block resonators," *IEEE Int. Electron Devices Meeting (IEDM'03),* pp. 39-3 (2003).
[4] S. Wang, L.C. Popa, D. Weinstein, "GaN MEMS resonator using a folded phononic crystal structure," *IEEE MEMS'15,* pp. 1028-31 (2015).
[5] A. Ansari, V.J. Gokhale, J. Roberts, M. Rais-Zadeh, "Gallium Nitride-on-Silicon micromechanical overtone resonators and filters," *IEEE Int. Electron Devices Meeting (IEDM'11)*, pp. 20.3.1-4. (2011).
[6] L.C. Popa, D. Weinstein, "L-Band Lamb mode resonators in Gallium Nitride MMIC technology," *IEEE Frequency Control Symposium (FCS'14),* pp. 1-4 (2014).
[7] B. Bahr, L.C. Popa, D. Weinstein, "1GHz GaN-MMIC monolithically integrated MEMS-based oscillators," *IEEE Int. Solid-State Circuits Conf. (ISSCC'15)*, pp. 1-3 (2015).
[8] A. Tazzoli, M. Rinaldi, G. Piazza, "Experimental investigation of thermally induced nonlinearities in Aluminum Nitride contour-mode MEMS resonators," *IEEE Electron Device Letters* 33(5), 724-726 (2012).

CONTACT

*Siping Wang : spinwang@mit.edu
*Dana Weinstein : dana@mtl.mit.edu